Chapter 13
Appendices

13.1 Appendix A: Rotating Bars, Paddles and Blades

Many practical applications involve bars or blades rotating around an axis, in which the body forces resulting from centrifugal loading generate internal stresses that must be kept under control. Take, for example, the solid bar shown in Fig. A.1, which has a circular cross section and rotates at angular velocity ω; the bar has the free edge, i.e. without end mass.

The elementary centrifugal force generated by a bar element of mass dm located between two cross sections of abscissa r and $r + dr$ relative to the rotational axis respectively is given by the relation:

$$dF = dm \cdot \omega^2 \cdot r = \gamma \cdot dV \cdot \omega^2 \cdot r = \gamma \cdot A \cdot \omega^2 \cdot r \cdot dr \tag{A.1}$$

where γ is the density of the bar material, dV is the elementary volume of the element in question, and A is the surface area of the cross section.

The resultant centrifugal force on a generic cross section at a distance r from the rotational axis and deriving from the body forces acting from r to L will thus be given by the relation:

$$F = \int_r^L \gamma \cdot A \cdot \omega^2 \cdot r \cdot dr = \gamma \cdot A \cdot \omega^2 \cdot \frac{\left(L^2 - r^2\right)}{2}. \tag{A.2}$$

It follows that the stress due to centrifugal load acting at radius r is given by:

$$\sigma_r = \frac{F}{A} = \gamma \cdot \omega^2 \cdot \frac{\left(L^2 - r^2\right)}{2}. \tag{A.3}$$

The maximum value of stress σ_r occurs for $r = 0$ and is $(\sigma_r)_{max} = \gamma \cdot \omega^2 \cdot L^2/2$.

V. Vullo and F. Vivio, *Rotors: Stress Analysis and Design*,
Mechanical Engineering Series, DOI 10.1007/978-88-470-2562-2_13,

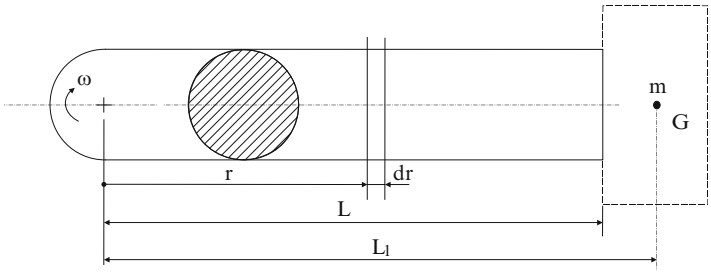

Fig. A.1 Solid cylindrical bar with circular cross section only rotating, with and without end mass

As we are dealing here with a uniaxial stress state, the total elongation of the portion of the rotating bar between generic axis r and the free end, where $r = L$, is given by the relation:

$$\ell = \int_r^L d\ell = \int_r^L \frac{\sigma_r}{E} \cdot dr = \int_r^L \gamma \cdot \omega^2 \cdot \frac{\left(L^2 - r^2\right)}{2E} \cdot dr. \tag{A.4}$$

Integrating this relation gives:

$$\ell = \frac{\gamma \cdot \omega^2}{2E} \cdot \left(\frac{2}{3} \cdot L^3 - L^2 \cdot r + \frac{r^3}{3}\right). \tag{A.5}$$

It follows from this relation that the total elongation of the bar occurs for $r = 0$ and is given by the relation:

$$\ell_t = \frac{\gamma \cdot \omega^2 \cdot L^3}{3 \cdot E}. \tag{A.6}$$

If a mass m whose center of gravity G is located at a distance L_1 from the rotational axis is connected to the end of the bar, as also shown in Fig. A.1, its effect must be taken into account. Consequently, relation (A.3) becomes:

$$\sigma_r = \gamma \cdot \omega^2 \cdot \frac{\left(L^2 - r^2\right)}{2} + \frac{m \cdot L_1 \cdot \omega^2}{A}. \tag{A.7}$$

We will now suppose that the solid bar has a conical profile and that its cross section is circular (Fig. A.2). Let A and A_0 be the surface areas of the cross sections at the generic distance r from the apex and at the rotational axis respectively. As these surface areas are clearly linked by the relation $A = A_0 \cdot r^2/L^2$, the elementary centrifugal force generated by a bar element of mass dm located between two cross sections of abscissa r and $r + dr$ relative to the apex respectively is given by the relation:

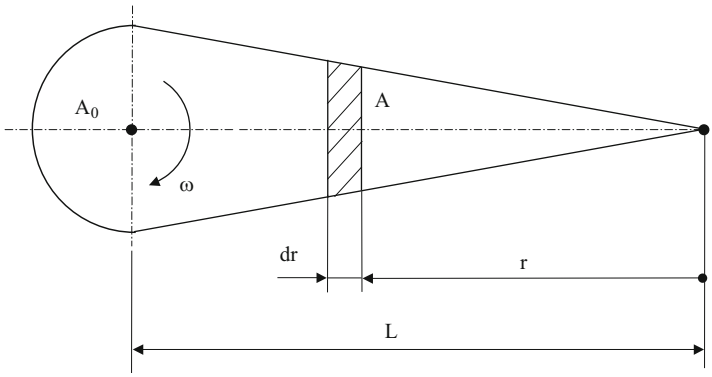

Fig. A.2 Solid conical bar with circular cross section only rotating

$$dF = dm \cdot \omega^2 \cdot (L - r) = \gamma \cdot dV \cdot \omega^2 \cdot (L - r)$$
$$= \gamma \cdot \omega^2 \cdot \left(A_0/L^2\right) \cdot (L - r) \cdot r^2 \cdot dr. \tag{A.8}$$

The resultant centrifugal force on a generic section at a distance $(L - r)$ from the rotational axis and deriving from the body forces acting from the apex $(r = 0)$ to the cross section of abscissa r will thus be given by the relation:

$$F = \frac{\gamma \cdot A_0 \cdot \omega^2}{L^2} \cdot \int_0^r (L - r) \cdot r^2 \cdot dr = \frac{\gamma \cdot A_0 \cdot \omega^2}{L^2} \cdot \left(\frac{L \cdot r^3}{3} - \frac{r^4}{4}\right). \tag{A.9}$$

It follows that the stress due to centrifugal load acting at the generic abscissa r is given by:

$$\sigma_r = \frac{F}{A} = \gamma \cdot \omega^2 \cdot \left(\frac{L \cdot r}{3} - \frac{r^2}{4}\right). \tag{A.10}$$

This stress assumes its maximum value for $r = L$, where it is $(\sigma_r)_{max} = \gamma \cdot \omega^2 \cdot L^2/12$.

The total elongation of the portion of the rotating bar between generic abscissa r and the apex is given by the relation:

$$\ell = \int_0^r d\ell = \int_0^r \frac{\sigma_r}{E} \cdot dr = \int_0^r \frac{\gamma \cdot \omega^2}{E} \cdot \left(\frac{L \cdot r}{3} - \frac{r^2}{4}\right) \cdot dr = \frac{\gamma \cdot \omega^2}{6 \cdot E}\left(L \cdot r^2 - \frac{r^3}{3}\right). \tag{A.11}$$

It follows from this relation that the total elongation of the bar is with $r = L$ and is:

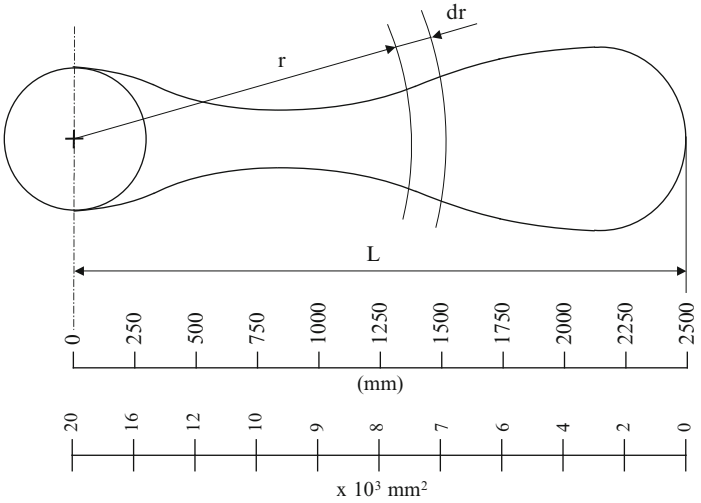

Fig. A.3 Rotating blade of given geometry

$$\ell_t = \frac{\gamma \cdot \omega^2 \cdot L^3}{12 \cdot E}. \tag{A.12}$$

If the rotating bar's profile cannot be expressed by a simple equation, it will not be possible to proceed analytically, as numerical methods or graphic procedures will be needed. The following example illustrates a procedure belonging to this latter family. We will consider the rotating blade shown in Fig. A.3, whose shape and the surface areas of the cross sections at predetermined distances r from the rotational axis are known. It will be assumed that the blade consists of aluminum and rotates at a velocity of 1,500 rpm.

The elementary centrifugal force generated by a blade element of mass dm located between two cross sections of abscissa r and $r + dr$ relative to the rotational axis respectively is given by the relation:

$$dF = \gamma \cdot A \cdot \omega^2 \cdot r \cdot dr. \tag{A.13}$$

where γ is the density of the material (for aluminum, $\gamma = 2{,}700$ kg/m^3) and A is the surface area of the cross section at the generic distance r from the rotational axis. The resultant centrifugal force on a generic cross section of abscissa r deriving from the body forces acting from r to L will thus be given by the relation:

$$F = \gamma \cdot \omega^2 \cdot \int_r^L A \cdot r \cdot dr. \tag{A.14}$$

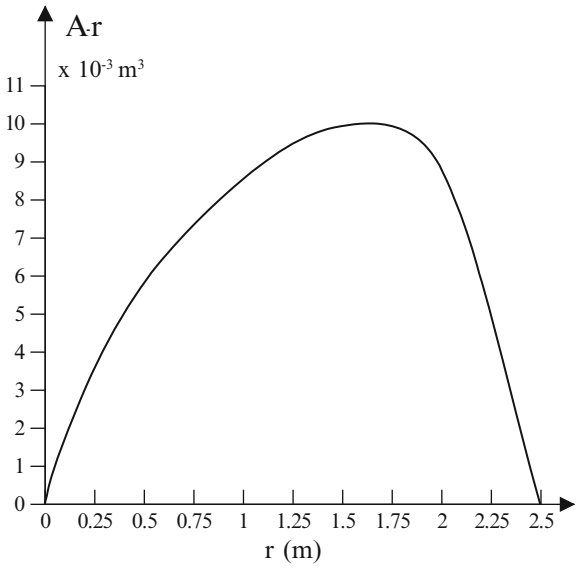

Fig. A.4 Product A·r versus radius r

When all magnitudes are expressed in consistent SI units (L and r in m, A in m^2, $\omega = 2\pi n/60 = 157$ rad/s), the foregoing relation becomes:

$$F = 6.655 \cdot 10^7 \cdot \int_r^{2.5} A \cdot r \cdot dr. \tag{A.15}$$

This relation is integrated graphically as follows. The product $A{\cdot}r$ is first plotted versus r, as shown in Fig. A.4. The centrifugal force acting on the generic cross section at distance r from the rotational axis is given by the area subtended by the portion of the curve between abscissa r and the end of the blade ($r = L$), multiplied by the factor $6.655{\cdot}10^7$. The stress σ_r due to centrifugal force in the generic cross section of area A is then obtained from the simple relation $\sigma_r = F/A$. Table A.1 summarizes the values of the magnitudes needed to calculated this stress.

The elongation of the portion of the blade between the generic cross section of abscissa r and the free end occurring as a result of centrifugal force is given by the relation:

$$\ell = \int_r^L \frac{\sigma_r}{E} \cdot dr = \frac{1}{E} \cdot \int_r^L \sigma_r \cdot dr. \tag{A.16}$$

The first step is to plot stress σ_r as a function of r as shown in Fig. A.5, after which this function is integrated graphically. Detailed calculation will be left to the

Table A.1 Numerical values of the magnitudes used to calculate radial stress σ_r

r	$A \cdot r$	$\int_r^{2.5} A \cdot r \cdot dr.$	$F = 6.655 \cdot 10^7 \cdot \int_r^{2.5} A \cdot r \cdot dr.$	$\sigma_r = \frac{F}{A}$
(m)	(10^{-3} m^3)	(10^{-3} m^4)	(MN)	(MPa)
0	0	17.47	1.163	58
0.25	4.0	16.97	1.129	71
0.50	6.0	15.72	1.046	87
0.75	7.5	14.03	0.934	94
1.00	9.0	11.97	0.797	89
1.25	10.0	9.72	0.647	81
1.50	10.5	7.16	0.475	68
1.75	10.5	4.53	0.302	50
2.00	8.0	2.22	0.148	37
2.25	4.5	0.66	0.044	22
2.50	0	0	0	0

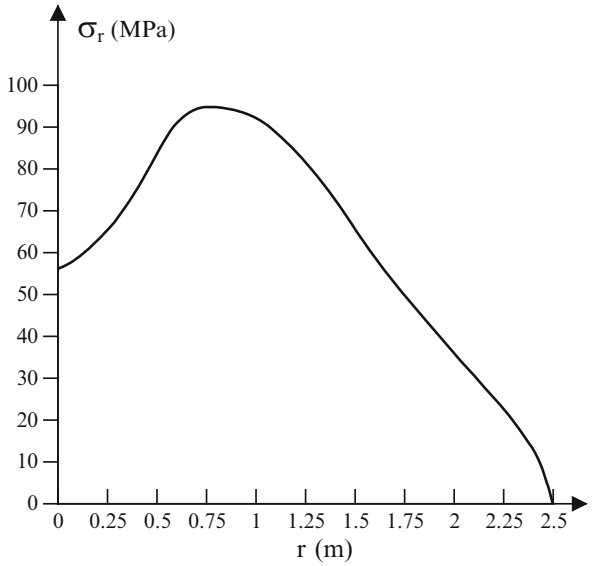

Fig. A.5 Stress σ_r versus radius r

reader. Noting that we have $E = 70$ GPa for aluminum, the resulting total elongation is thus:

$$\ell = \frac{1}{E} \cdot \int_0^{2.5} \sigma_r \cdot dr = 2.24 \cdot 10^{-3}\text{m}.$$

13.2 Appendix B: In-Depth Analysis of the Solution of the Hypergeometric Differential Equation

Both Honegger and Giovannozzi note that: (1) the independent integrals u_1 and u_2 are convergent within the interval $0 < t < 1$; (2) convergence decreases as t increases and, starting around $t = 1/2$, several terms of the series expansion are needed to calculate the function value with suitable accuracy; (3) with even higher t values, calculation becomes more intricate, especially in view of the calculation tools available at the time these authors wrote. Accordingly, both split the interval $0 < t < 1$ into two contiguous parts $0 < t \leq 1/2$ and $1/2 < t < 1$ bounded by $t = 1/2$, and use the integral u_1 and a linear combination of the two independent integrals u_1 and u_2 in the interval $0 < t \leq 1/2$, whereas in the interval $1/2 < t < 1$ they make use of other solutions of associated homogeneous equation (6.6) based on two different independent integrals expressed by means of power series in the variable $x = (1 - t)$.

By introducing this new variable, the differential equation (6.6) becomes:

$$\frac{d^2u}{dx^2} + \left(\frac{1}{x} + \frac{1}{x-1}\right) \cdot \frac{du}{dx} + \left[-(1-v) - \frac{1}{x-1}\right] \cdot \frac{u}{x \cdot (x-1)} = 0 \qquad \text{(B.1)}$$

This is still a hypergeometric differential equation, again featuring three singularity points ($x = 0$; $x = 1$; $x = \infty$), and corresponding to the general form:

$$\frac{d^2u}{dx^2} + \left(\frac{1-\alpha-\alpha'}{x} + \frac{1-\gamma-\gamma'}{x-1}\right) \cdot \frac{du}{dx} + \left[-\frac{\alpha \cdot \alpha'}{x} + \frac{\gamma \cdot \gamma'}{x-1} + \beta \cdot \beta'\right] \cdot \frac{u}{x \cdot (x-1)} = 0 \qquad \text{(B.2)}$$

As this has the same structure as (6.16), applying the procedure described earlier to it allows us to conclude that its integrals are the same as those given by relations (6.20), after substituting factors α and α' with γ and γ'respectively, while β and β' remain unchanged. As a result of the variable change $x = (1 - t)$, the three singularity points of variable t ($t = 0$; $t = 1$; $t = \infty$) correspond respectively to as many singularity points of variable x ($x = 0$; $x = 1$; $x = \infty$). In other words, using Riemann's notation, the following can be specified:

$$P\begin{pmatrix} 0 & \infty & 1 & \\ \alpha & \beta & \gamma & t \\ \alpha' & \beta' & \gamma' & \end{pmatrix} = P\begin{pmatrix} 1 & \infty & 0 & \\ \alpha & \beta & \gamma & x \\ \alpha' & \beta' & \gamma' & \end{pmatrix} = P\begin{pmatrix} 0 & \infty & 1 & \\ \gamma & \beta & \alpha & x \\ \gamma' & \beta' & \alpha' & \end{pmatrix}. \qquad \text{(B.3)}$$

The first independent integral $\bar{u}_1$ in (6.6) will thus be expressed in the following form:

$$\begin{aligned}\bar{u}_1 &= (1-x)\cdot F(\gamma'+\beta+\alpha, \gamma'+\beta'+\alpha, 1-\gamma'-\gamma, x) = (1-x)\cdot F(a,b,c,x) = \\ &= (1-x)\cdot F\left(\frac{3}{2}+\xi, \frac{3}{2}-\xi, 1, x\right) = \\ &= (1-x)\cdot\left[1+\frac{\left(\frac{3}{2}+\xi\right)\cdot\left(\frac{3}{2}-\xi\right)}{1!\cdot 1}\cdot x+\frac{\left(\frac{3}{2}+\xi\right)\cdot\left(\frac{3}{2}+\xi+1\right)\cdot\left(\frac{3}{2}-\xi\right)\cdot\left(\frac{3}{2}-\xi+1\right)}{2!\cdot 1\cdot 2}\cdot x^2+\ldots\right]\end{aligned} \tag{B.4}$$

which, reintroducing variable t, becomes:

$$\bar{u}_1 = \quad t\cdot F\left(\frac{3}{2}+\xi, \frac{3}{2}-\xi, 1, [1-t]\right) \tag{B.5}$$

Here again, the second independent integral $\bar{u}_2$ must be calculated with a domain change of the independent variable, as we are again dealing with factors in the hypergeometric series that assume infinite value. With a procedure similar to that used in Sect. 6.2.2 to calculate u_2, it can be demonstrated that the following expression can be used for $\bar{u}_2$:

$$\bar{u}_2 = \bar{u}_1\cdot\ln x + (1-x)\cdot\sum_{i=1}^{\infty}\bar{C}_i\cdot x^i = \bar{u}_1\cdot\ln(1-t) + t\cdot\sum_{i=1}^{\infty}\bar{C}_i\cdot(1-t)^i \tag{B.6}$$

where

$$\bar{C}_i = \frac{\prod_{m=1}^{i}\left(\frac{3}{2}+\xi+m-1\right)\cdot\left(\frac{3}{2}-\xi+m-1\right)}{i!\cdot i!}\cdot\sum_{m=0}^{i-1}\left(\frac{1}{\frac{3}{2}+\xi+m}+\frac{1}{\frac{3}{2}-\xi+m}-\frac{2}{1+m}\right). \tag{B.7}$$

With the procedure used by Honegger and by Giovannozzi, two pairs of independent integrals are found for the homogeneous differential equation 6.6, the first (u_1 and u_2) being valid within the interval $0 \le t \le 1/2$ and the second ($\bar{u}_1$ and $\bar{u}_2$) valid within the interval $1/2 < t \le 1$. However, it can readily be seen that at point $t = 1/2$ separating the two contiguous parts of the interval, the domain of the internal integrals u_1 and u_2 does not match the domain of the two external integrals $\bar{u}_1$ and $\bar{u}_2$. Continuity of integral u_1 beyond $t = 1/2$ up to $t = 1$ can be obtained by means of a linear combination of $\bar{u}_1$and $\bar{u}_2$, given that any linear combination of two independent integrals is sufficient solution to satisfy the differential equation in question.

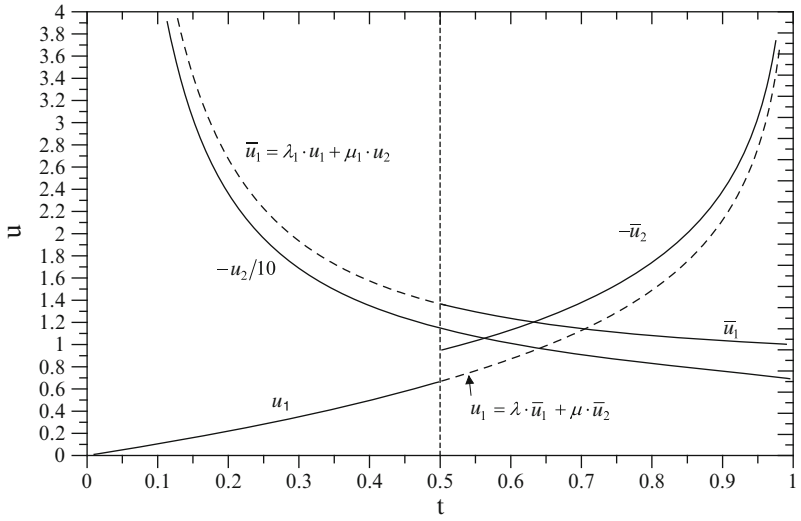

Fig. B.1 Functions u_1 and $\bar{u}_1$ used by Honegger and Giovannozzi for conical disks, and functions u_2 and $\bar{u}_2$

In this connection, Honnegger and Giovannozzi define two constants λ and μ, so that, for $t = 1/2$, the continuity of the function and of its first derivative are satisfied, in order to have:

$$\begin{aligned} u_1 &= \lambda \cdot \bar{u}_1 + \mu \cdot \bar{u}_2 \\ \frac{du_1}{dt} &= \lambda \cdot \frac{d\bar{u}_1}{dt} + \mu \cdot \frac{d\bar{u}_2}{dt}. \end{aligned} \tag{B.8}$$

A relation is thus obtained – the first of relations (B.8) – whereby u_1 can be calculated beyond $t = 1/2$, i.e., within the interval of independent variable $1/2 < t \leq 1$. Similarly, and again following the procedure outlined by Honegger and Giovannozzi, a function $\bar{u}_1 = \lambda_1 \cdot u_1 + \mu_1 \cdot u_2$ expressed as a linear combination of u_1 and u_2 can be found by using two new constants λ_1 and μ_1. This function is valid within the interval $0 \leq t \leq 1/2$.

To summarize, both Honegger and Giovannozzi split the interval $0 \leq t \leq 1$ into two component partial intervals $0 \leq t \leq 1/2$ and $1/2 < t \leq 1$ and, as shown in Fig. B.1, use integral u_1 obtained from relation (6.22) within the interval $0 \leq t \leq 1/2$, and linear combination $u_1 = \lambda \cdot \bar{u}_1 + \mu \cdot \bar{u}_2$ obtained from the first relation (B.8) within the interval $1/2 < t \leq 1$. In addition, they use integral $\bar{u}_1$ obtained from relation (B.5) within the interval $1/2 \leq t \leq 1$, and linear combination $\bar{u}_1 = \lambda_1 \cdot u_1 + \mu_1 \cdot u_2$(equivalent to the first relation (B.8)), with λ_1 and μ_1 as constants to be found by imposing the continuity of the function and its first derivative at point $t = 1/2$, within the interval $0 \leq t < 1/2$. Both researchers express the

solution of the associated homogeneous equation (6.6) as a linear combination of the two independent integrals, viz.:

$$u = C_1 \cdot u_1 + C_2 \cdot \bar{u}_1, \tag{B.9}$$

where C_1 and C_2 are integration constants to be determined by imposing boundary conditions, whereas $u_1$and $\bar{u}_1$feature different expressions depending on whether the interval $0 \leq t \leq 1/2$ or the interval $1/2 < t \leq 1$ applies.

Lastly, it should be noted that, as shown in Fig. 6.1b, e, f, g the function $h = h_0 \cdot (1 - t)$ can also describe the geometry of diverging conical disks. In the general case where the apex V does not converge on the axis (Fig. 6.1e, f, g) and $t > 1$, it is advisable to introduce the new variable $y = 1/t$, as does Giovannozzi, to solve (6.6) analytically. By replacing this variable in (6.6), a hypergeometric differential equation is found which is formally similar to (6.16) and (B.1). By following the same procedure used for these two equations, we again reach the conclusion that the integrals of the hypergeometric differential equation thus obtained are the same as those given by relations (6.20), after substituting factors α and $\alpha'$with β and β', while γ and γ' remain unchanged. As a result of the variable change $y = 1/t$, the three singularity points of variable t ($t = 0$; $t = 1$; $t = \infty$) correspond respectively to as many singularity points of variable y ($y = \infty$; $y = 1$; $y = 0$). In this case, using Riemann's notation, the following can be specified:

$$P\begin{pmatrix} 0 & \infty & 1 & \\ \alpha & \beta & \gamma & t \\ \alpha' & \beta' & \gamma' & \end{pmatrix} = P\begin{pmatrix} \infty & 0 & 1 & \\ \alpha & \beta & \gamma & y \\ \alpha' & \beta' & \gamma' & \end{pmatrix} = P\begin{pmatrix} 0 & \infty & 1 & \\ \beta & \alpha & \gamma & y \\ \beta' & \alpha' & \gamma' & \end{pmatrix}. \tag{B.10}$$

We will not discuss the further developments (which are entirely similar to those that have been described) or the procedures involved in introducing new variables related to variable t in order to improve calculation of hypergeometrical series, as does Giovannozzi, in specific sub-intervals of interval $1 < t < \infty$.

Where the conical disc has lateral faces converging on the axis of rotation (see Fig. 4.1a), it is in any case preferable to calculate stress and strain states by means of a closed form formulation based on Stodola's hyperbolic profile disk.

13.3 Appendix C: The Finite Element Method for Elastic-Plastic Problems

Many structural problems involve nonlinearities, which may be both geometric and in the material's behavior. The latter include cases where, as a result of applied loads, stress and strain states are generated in the material that exceed the non-linear elastic limits, so that the material is stressed beyond yielding. With the finite element method, all nonlinear problems, regardless of the nature of the nonlinearities, are generally solved by reducing them to a sequence of linear steps.

The procedure thus involves writing the equilibrium equations $\{Q\} = [K]\{\delta\}$ in the following incremental form:

$$\{\Delta Q\} = [K]\{\Delta\delta\} \tag{C.1}$$

where $\{\Delta Q\}$ is the total or equivalent nodal force increment matrix, and the stiffness matrix $[K]$ is a function of displacements $\{\delta\}$, as the problem is nonlinear. In the following steps, the current vector $\{\delta\}$ is the sum of the previous vectors $\{\Delta\delta\}$, while the current matrix $[K]$, called the *tangent stiffness matrix*, is used to calculate the next step $\{\Delta\delta\}$. The vector $\{\delta\}$ and the matrix $[K]$ are then updated, and we are ready to perform another step. With this process, the true stress-true strain curve is approximated by means of a succession of straight segments.

As we know from *continuum mechanics*, if the stress-strain relationships are linear or nonlinear but still elastic, there is a one-to-one correspondence between stress and strain. By contrast, if there are plastic deformations, this correspondence will no longer be one-to-one, as any given stress state can be produced by many different strain paths. As the focus here is on plasticity, we will ignore the effects of other nonlinearities such as the geometric nonlinearities resulting from large deformations. The algorithms used to solve these problems are in any case entirely general, and apply independently of the nature of the nonlinearities exhibited.

Solving plastic problems with the finite element method is based on the Levy-Mises plasticity theory, which is an *incremental theory* or *plastic flow theory*, as it relates stress increments to strain increments. According to this theory, the increment of equivalent or effective plastic strain $d\varepsilon_e^p$ is defined by the contributions of the single, separate increments of plastic strain and is expressed with reference to a three-dimensional rectangular system O(x, y, z) of non-principal axes in the form:

$$d\varepsilon_e^p = \frac{\sqrt{2}}{3}\left\{\left(d\varepsilon_x^p - d\varepsilon_y^p\right)^2 + \left(d\varepsilon_y^p - d\varepsilon_z^p\right)^2 + \left(d\varepsilon_z^p - d\varepsilon_x^p\right)^2 + \frac{3}{2}\left[\left(d\gamma_{xy}^p\right)^2 + \left(d\gamma_{yz}^p\right)^2 + \left(d\gamma_{zx}^p\right)^2\right]\right\}^{1/2}, \tag{C.2}$$

where index p, in addition to the other subscripts of known meaning, denotes the plastic contribution. In accordance with the Von Mises criterion for triaxial stress, and again with reference to the system of non-principal axes, yielding begins when the equivalent or effective stress σ_e reaches and exceeds a specific limit value; σ_e is given by the relation:

$$\sigma_e = \frac{\sqrt{2}}{2}\left[\left(\sigma_x - \sigma_y\right)^2 + \left(\sigma_y - \sigma_z\right)^2 + \left(\sigma_z - \sigma_x\right)^2 + 6\left[\tau_{xy}^2 + \tau_{yz}^2 + \tau_{zx}^2\right]\right]^{1/2}. \tag{C.3}$$

With reference to the uniaxial tensile test, beyond yielding, or in other words in the plastic range where Poisson's ratio ν is 0.5, we have:

$$\sigma_e = \sigma_x \quad \text{and} \quad d\varepsilon_e^p = d\varepsilon_x^p \tag{C.4}$$

In the $\sigma_e = \sigma_e(\varepsilon_e)$ curve shown in Fig. 12.3a, P represents the onset of yielding ($\sigma = \sigma_s$); for $\sigma = \sigma_A$, with $\sigma_A > \sigma_s$, the total equivalent strain ε_e is the sum of elastic strain ε_e^e, which can be completely recovered when load is removed, and plastic strain ε_e^p, i.e., $\varepsilon_e = \varepsilon_e^e + \varepsilon_e^p$. The material hardens as a result of plastic strain ε_e^p. If the specimen is loaded again, further yielding will not take place until σ_e exceeds σ_A. It is assumed that yielding will occur for $\sigma_e > \sigma_A$ regardless of the type of stress considered (i.e., tensile, compressive or multiaxial), i.e., that the material anisotropy effects generated by plastic deformation – including the Bauschinger effect described earlier – can be neglected. In other words, the isotropic strain hardening criterion is considered to apply.

As we saw in Sect. 12.3, the slope H' at any point of the $\sigma_e = \sigma_e\left(\varepsilon_e^p\right)$ curve (Fig. 12.3b) is given by relation (12.33). The increments of equivalent stresses, of total strains and of plastic strains are given by the following relations, which all involve 6×1 vectors:

$$\begin{aligned} \{d\sigma_e\} &= \left\{d\sigma_x, d\sigma_y, ..., d\tau_{zx}\right\} \\ \{d\varepsilon_e\} &= \left\{d\varepsilon_x, d\varepsilon_y, ..., d\gamma_{zx}\right\} \\ \left\{d\varepsilon_e^p\right\} &= \left\{d\varepsilon_x^p, d\varepsilon_y^p, ..., d\gamma_z^p\right\}. \end{aligned} \tag{C.5}$$

The deviatoric stresses s_x, s_y, ..., are defined by the relations:

$$\begin{aligned} s_x &= \sigma_x - \sigma_m; \quad & s_y &= \sigma_y - \sigma_m; \quad & s_z &= \sigma_z - \sigma_m; \\ s_{xy} &= \tau_{xy}; & s_{yz} &= \tau_{yz}; & s_{zx} &= \tau_{zx}; \end{aligned} \tag{C.6}$$

where $\sigma_m = \left(\sigma_x + \sigma_y + \sigma_z\right)/3$ is the average stress. By differentiating relation (C.3), we then obtain:

$$d\sigma_e = \{R\}^T\{d\sigma\} \quad \text{where} \quad \{R\} = \frac{3}{\sigma_e}\left\{\frac{s_x}{2} \quad \frac{s_y}{2} \quad \frac{s_z}{2} \quad s_{xy} \quad s_{yz} \quad s_{zx}\right\} \tag{C.7}$$

It should be noted here that $\sigma_e^2 = 9\tau_{oct}^2/2 = 3J_2$, where τ_{oct} is the octahedral shear stress and J_2 is the second invariant of the deviatoric stresses. The theory used here is also called the J_2 *flow theory*. It should also be borne in mind that the flow rule associated with the Von Mises yield criterion is represented by the Prandtl-Reuss relation, which states that:

$$d\varepsilon^p = \{R\}d\varepsilon_e^p. \tag{C.8}$$

This means that there will be increments of plastic strain $\{d\varepsilon^p\}$ when an increment of equivalent plastic strain $d\varepsilon_e^p$ occurs as the result of a stress state $\{R\}$. The corresponding stress increment $\{d\sigma\}$ can be written as a function of the increments of elastic strain $\{d\varepsilon^e\}$ in the following shape:

$$\{d\sigma\} = [E]\{d\varepsilon^e\} \text{ or } \{d\sigma\} = [E]\left(\{d\varepsilon^*\} - \{d\varepsilon^p\}\right) \tag{C.9}$$

with

$$\begin{aligned} \{d\varepsilon^e\} &= \{d\varepsilon\} - \{d\varepsilon^p\} - \{d\varepsilon^T\} - \{d\varepsilon^C\} \text{ and} \\ \{d\varepsilon^*\} &= \{d\varepsilon\} - \{d\varepsilon^T\} - \{d\varepsilon^C\} \end{aligned} \tag{C.10}$$

where $[E]$ is the conventional matrix of elastic constants, while the five strain vectors appearing in the first relation (C.10) represent the increments of elastic, total, plastic, thermal (or initial) and creep strains respectively. Obviously, if there is no contribution from thermal loading or creep, we must put $\{d\varepsilon^T\} = 0$ and $\{d\varepsilon^C\} = 0$ in this relation.

With the finite element method, we first determine the vector $\{d\varepsilon\}$. Relations (C.8) and (C.9) can be used to find the vector $\{d\sigma\}$ only after $d\varepsilon_e^p$ has been calculated. To find $d\varepsilon_e^p$, relation (C.8) is substituted in (C.9) and both members of the relation thus found are premultiplied by $\{R\}^T$. We then substitute $\{R\}^T\{d\sigma\} = H'\, d\varepsilon_e^p$, as obtained from relations (C.4), (12.34) and (C.7), and obtain:

$$d\varepsilon_e^p = [W]\{d\varepsilon^*\} \text{ with } [W] = \frac{\{R\}^T[E]}{H' + \{R\}^T[E]\{R\}} \tag{C.11}$$

Substituting relation (C.11) in (C.8) and the result thus found in relation (C.9) gives the following incremental stress-strain relation, similar to the elastic relation $\{\sigma\} = [E]\,\{\varepsilon\}$, but applying to elasto-plastic behavior:

$$\{d\sigma\} = [E^*]\left(\{d\varepsilon\} - \{d\varepsilon^T\} - \{d\varepsilon^C\}\right) = [E^*]\{d\varepsilon^*\} \tag{C.12}$$

where

$$[E^*] = [E] - [E]\{R\}[W] \tag{C.13}$$

Matrix $[E^*]$ is symmetric and also applies for elastic-perfectly plastic materials, for which $E_T = H' = 0$ (Fig. 12.3).

In linear elastic problems, stresses and strains depend on load, but not on how the load state is reached: in other words, the sequence of loads is not important. In elastic-plastic problems, on the other hand, the results depend on the loading sequence. Loading is considered proportional when the stresses at any point of the continuum in question maintain the same ratio to one another throughout loading.

The assumption of isotropic strain hardening holds true for proportional loads. For non-proportional loads, as for loads that change sign, this assumption is less

valid, though it is still a sufficiently satisfactory approximation for many problems involved in practical applications. Other strain hardening criteria lead to different matrixes $[E^*]$; in this connection, it should be noted that a number of models have attempted to unify and generalize the strain hardening criteria, even in cases where softening phenomena are also involved.

It should also be borne in mind that plasticity is independent of time. The equations involved are often written in terms of rate, with the sole purpose of highlighting the nature of plastic flow. Thus, for example, (C.8) becomes $\{\dot{\varepsilon}^p\} = \{R\}\{\dot{\varepsilon}_e^p\}$. This, however, is a topic that goes beyond our scope here.